TRANSMISSION OF INTERIOR CONCRETE COLUMN LOADS THROUGH FLOORS

Reference 10.44

By Carlos E. Ospina,[1] Associate Member, ASCE, and Scott D. B. Alexander[2]

ABSTRACT: Clause 10.15.3 of the 1995 ACI code (ACI 318-95) defines the effective strength of a high-strength concrete interior column with an intervening normal strength concrete slab. This provision is based on laboratory tests in which no load was applied to the slab. Such tests may overestimate the strength of the column because they do not properly model the confinement conditions of the column-slab joint. This paper reports experimental results of tests with properly modeled confinement conditions. The test results show that the intensity of slab load, the aspect ratio of the joint, and the rectangularity of the column affect the strength of an interior column-slab joint. A new design equation replacing the provision in Clause 10.15.3 is proposed.

INTRODUCTION

For reasons of economy, concrete columns are often made with higher-strength concrete than are the flab slabs or plates they support. In the preferred method of construction, the slab concrete is cast continuous through the column-slab joint. As a result, that part of the column forming the joint between the slab and the column is made with a lower grade of concrete than is the rest of the column.

Section 10.15 of the ACI 318-95 ("Building code" 1995) offers three design strategies for the transmission of column loads through floors. The first involves placing high-strength concrete (HSC) in the column-slab joint and beyond, extending at least 600 mm into the slab. This method, called puddling or mushrooming, brings with it the logistical problem of casting a slab with two different grades of concrete. One can avoid this problem by casting the entire slab with high-strength concrete, but the design requirements of the slab may not justify the added expense of high-strength concrete. The second approach is to compensate for the lower-strength joint concrete by providing compression reinforcement. The disadvantage of this method is that it places additional reinforcement in a region that is already likely to be heavily reinforced.

Clause 10.15.3 presents a third strategy for cases where the column-slab joint is confined on all sides by slab. This approach, which is the subject of this paper, is to design the column-slab joint using an "effective" concrete strength. Because the joint is confined to some degree by the surrounding slab, the effective strength of the joint concrete is higher than its cylinder strength. However, this paper will show that the expression for effective strength given in the 1995 ACI code may be unsafe, as it is based on tests that do not properly model the confinement condition at the joint. Based on new test data, this paper presents a revised expression for the effective strength of an interior column-slab joint.

BACKGROUND

There are relatively few tests of interior column-slab joints reported in the literature. All existing results are for tests of joints with unloaded slabs. Bianchini et al. (1960) tested 11 interior column-slab joint specimens, and Gamble and Klinar (1991) tested six specimens with high-strength concrete columns. Details of these specimens are summarized in Table 1.

The traditional approach to the problem has been to treat the column-slab joint as part of the column. Both the ACI (1995) and CSA A23.3-94 ("Design" 1994) concrete design standards define the cross-sectional capacity, P_0, of a column under concentric load as

$$P_0 = \alpha_1 f'_c(A_g - A_{st}) + f_y A_{st} \tag{1}$$

where A_g is the gross area of the column, A_{st} is the area of longitudinal reinforcement, f'_c is the concrete cylinder strength, and f_y is the yield strength of the steel. In the ACI code, the factor α_1 is a constant equal to 0.85. In the Canadian standard, the factor α_1 is a variable dependent on the concrete strength.

In presenting their results, Bianchini et al. (1960) rearranged (1) to define an effective column strength, f'_{ce}:

$$f'_{ce} = \frac{P_{test} - f_y A_{st}}{\alpha_1(A_g - A_{st})} \tag{2}$$

where P_{test} is the maximum load carried by the test specimen.

The justification for including the factor α_1 in (2) is the desirability of designing column-slab joints using (1). The effective strength, f'_{ce}, is notionally the cylinder strength of some hypothetical concrete that combines the properties of the column and slab concrete. For consistency with previous studies, the test results in this investigation will be prepared using (2) with α_1 equal to 0.85.

The effective concrete strength defined by the 1995 ACI code is based on the results of Bianchini et al. (1960). For an interior column, the effective concrete strength is given by

$$\frac{f'_{cc}}{f'_{cs}} \le 1.4; \quad f'_{ce} = f'_{cc} \tag{3a}$$

$$\frac{f'_{cc}}{f'_{cs}} > 1.4; \quad f'_{ce} = 0.75 f'_{cc} + 0.35 f'_{cs} \tag{3b}$$

Gamble and Klinar (1991) found that this design provision overestimates the strength of joints in which the ratio of the column strength to the slab strength is large. They propose the following as a lower bound relationship for interior columns:

$$\frac{f'_{cc}}{f'_{cs}} \le 1.4; \quad f'_{ce} = f'_{cc} \tag{4a}$$

$$\frac{f'_{cc}}{f'_{cs}} > 1.4; \quad f'_{ce} = 0.47 f'_{cc} + 0.67 f'_{cs} \tag{4b}$$

Note that the two segments of the design curve proposed by Gamble and Klinar do not meet at a value of f'_{cc}/f'_{cs} equal to 1.4.

In extending design provisions to cover high-strength con-

[1]Grad. Student, Dept. of Civ. and Environ. Engrg., Univ. of Alberta, Edmonton, Alta., Canada T6G 2G7.

[2]Assoc. Prof., Dept. of Civ. and Environ. Engrg., Univ. of Alberta, Edmonton, Alta., Canada T6G 2G7.

Note. Associate Editor: Walter Gerstle. Discussion open until November 1, 1998. To extend the closing date one month, a written request must be filed with the ASCE Manager of Journals. The manuscript for this paper was submitted for review and possible publication on August 4, 1997. This paper is part of the ***Journal of Structural Engineering***, Vol. 124, No. 6, June, 1998. ©ASCE, ISSN 0733-9445/98/0006-0602–0610/ $8.00 + $.50 per page. Paper No. 16365.

TABLE 1. Brief Description of Interior Slab-Column Joint Specimens Found in Literature

Source (1)	Dimensions[a] (mm) a^b (2)	b^b (3)	c (4)	e (5)	h (6)	Column concrete strength (MPa) (7)	Slab concrete strength (MPa) (8)	Approximate Reinforcement ρ_{col} (9)	ρ_{slab} (10)
Bianchini et al. (1960)	788	788	279	635	178	22.5 ~ 53.4	13.4 ~ 23.6	1.46	0.45–0.54
Gamble and Klinar (1991)	1,067	1,067	254	610	127, 128	72.4 ~ 98.6	17.2 ~ 42.7	1.76	0.71–0.97

[a]Dimensions a through h are defined in Fig. 3.
[b]Dimensions a and b are equal since no holes were left in the slab segments.

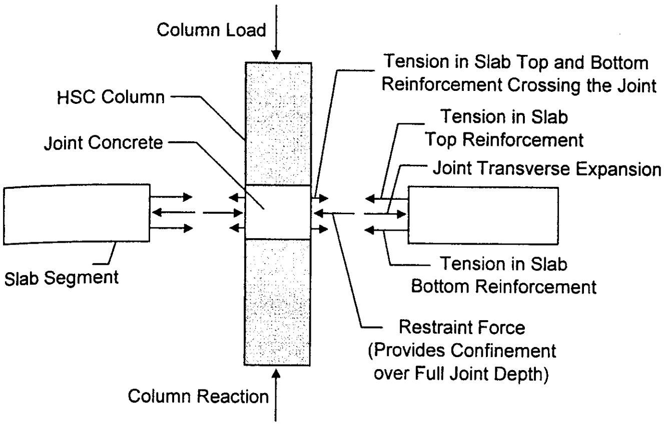

FIG. 1. Free Body Diagram of Specimen with Unloaded Slab

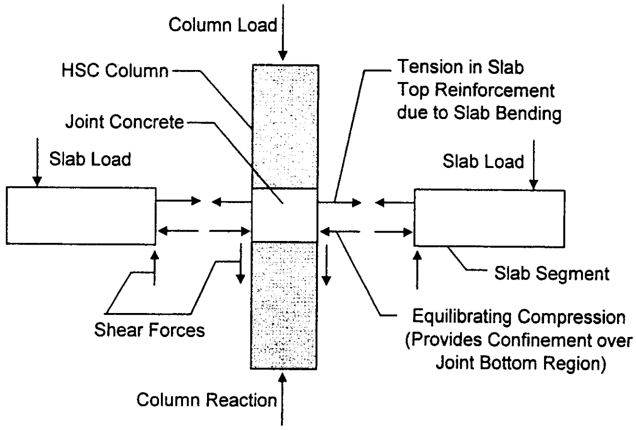

FIG. 2. Free Body Diagram of Specimen with Loaded Slab

crete, the Canadian standard (1994) presents the following expression for interior columns:

$$\frac{f'_{cc}}{f'_{cs}} \leq 1.4; \quad f'_{ce} = f'_{cc} \tag{5a}$$

$$\frac{f'_{cc}}{f'_{cs}} > 1.4; \quad f'_{ce} = 0.25f'_{cc} + 1.05f'_{cs} \tag{5b}$$

A striking feature of the test programs by both Bianchini et al. (1960) and Gamble and Klinar (1991) is the absence of slab load. In a prototype structure, service load on the slab will produce significant tensile straining of the top mat flexural reinforcement in the vicinity of the column. It would seem reasonable to assume that such strain will have a detrimental effect on the ability of the surrounding slab to confine the column-slab joint.

Consider a column-slab joint in which the column concrete is stronger and stiffer than the slab concrete. Under load, the joint concrete can be expected to strain more than the column concrete. Lateral expansion of the joint, however, is constrained by the surrounding slab. If the surrounding slab is itself unloaded, as illustrated in Fig. 1, it will act as a tension band, restraining the lateral expansion of the joint and providing a passive confining pressure to the joint concrete. The confining pressure is distributed almost uniformly over the height of the joint, and tension is induced in both the top and bottom slab reinforcement. If the slab is loaded, as illustrated in Fig. 2, the bending of the slab places the upper portion of the joint in tension and the lower portion in compression. Below the neutral axis of bending, the flexural compression block of the slab actively confines the joint. Above the neutral axis of bending, the joint is essentially unconfined by the surrounding slab.

In addition to the confinement provided by the slab, the joint is restrained by shear stresses at the interfaces between the high-strength column concrete and the lower-strength joint concrete. This is analogous to the restraint provided by stiff loading platens when testing concrete cylinders and cores. The significance of this interface shear restraint will be greatest for joints in which the slab is thin relative to the dimension of the column. Gamble and Klinar (1991) suggested that the strength of a column-slab joint would be affected by its aspect ratio, the ratio of the slab thickness to the column dimension. However, there is little variation in the gross geometry of the existing body of test results. All test specimens feature square columns with joint aspect ratios from 0.5 to 0.7. There are no tests of joints with rectangular columns.

Assuming a typical slab thickness of 150 mm and a minimal column dimension of 300 mm, the joint aspect ratio for a two-way flat plate supported on square columns will be less than 0.5. However, slab drop panels and rectangular columns may produce aspect ratios as large as 1.0. Slabs with beams may have even larger joint aspect ratios but the differences between the flexural behavior of flat slabs and slabs with beams should reduce the impact of joint aspect ratio.

EXPERIMENTAL PROGRAM

The experimental work described here formed part of a larger investigation into the behavior of column-slab joints. The complete investigation is documented in Ospina and Alexander (1997).

Twenty interior column-slab joints in two series were tested to failure. The principal difference between the two series is the extent of instrumentation. Series A comprised pilot tests designed to examine primarily the effect of slab load on the strength of the column-slab joint. Four sets of specimens with three specimens in each set were tested to failure. The results of this series indicate that the effective strength of the joint is a function not only of the slab and column concrete strengths but also of the thickness of the slab relative to the column, expressed as the ratio h/c. Series B examined the effect of aspect ratio, h/c, and column rectangularity and provided measurements of the deformations in the column-slab joint.

Description of Specimens and Test Apparatus

Each specimen consisted of a reinforced concrete slab of normal strength sandwiched between two high-strength con-

TABLE 2. Details of Test Specimens

Specimen	Dimensions (mm)						Concrete Strength (MPa)[a]	
Mark (1)	a (2)	b (3)	c (4)	d[b] (5)	e (6)	h (7)	f'_{cc} (8)	f'_{cs} (9)
A1-A, B, C	1,380	1,100	200	75	500	100	105 (27)	40 (28)
A2-A, B, C	1,380	1,100	200	75	500	100	112 (29)	46 (28)
A3-A, B, C	1,380	1,100	200	125	500	150	89 (27)	25 (28)
A4-A, B, C	1,380	1,100	200	125	500	150	106 (29)	23 (28)
B-1	1,350	1,150	250	225	625	250	104 (51)	42 (49)
B-2	1,350	1,150	250	125	675	150	104 (56)	42 (54)
B-3[c]	1,350	1,150	250	225	625	250	113 (44)	44 (42)
B-4	1,350	1,150	250	125	675	150	113 (45)	44 (43)
B-5	1,350	1,150	250	225	625	250	95 (17)	15 (20)
B-6	1,350	1,150	250	125	675	150	95 (18)	15 (21)
B-7[d]	1,350	1,150	175 × 350	225	625	250	120 (21)	19 (23)
B-8[d]	1,350	1,150	175 × 350	125	675	150	120 (22)	19 (24)

[a]Numbers in parenthesis indicate age of column and slab concrete in days at time of testing.
[b]Measured from slab soffit to top slab reinforcement mat based on a nominal 20 mm slab concrete cover.
[c]Specimen with built-in high-strength concrete core.
[d]Specimens B-7 and B-8 had rectangular columns.

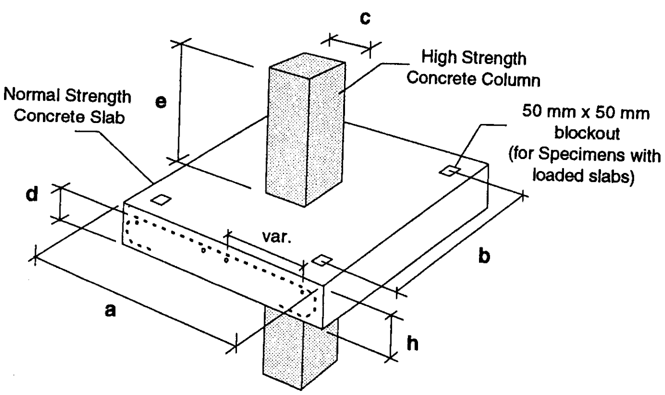

FIG. 3. Geometry of Test Specimens

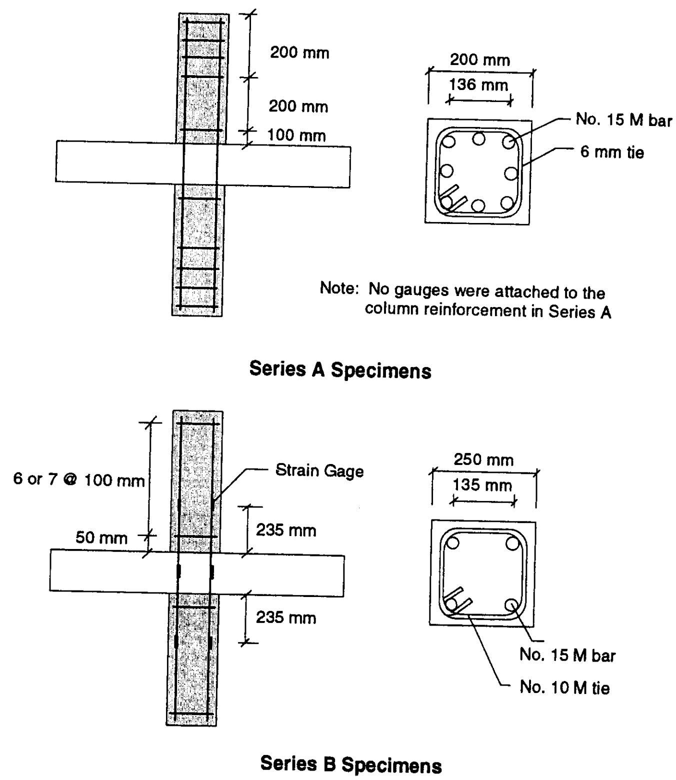

FIG. 4. Column Reinforcement and Strain Gauge Layout

crete column stubs, as shown in Fig. 3. Two specimens had rectangular columns; the remaining 18 had square columns. Dimensions and reinforcement quantities for each specimen are given in Table 2.

Elevations of the columns for series A and B are shown in Fig. 4. Column reinforcement was continuous for the full height of the specimen. The column bars were cut to the appropriate length but were not specially detailed for bearing. To improve load transfer at these column bar cutoffs, each column stub was capped with a reusable steel shoe that fully confined the end region. Slab flexural reinforcement is shown in Fig. 5.

Each specimen was cast in three stages: first the lower column stub, then the slab, and finally the upper column stub. The entire casting process took from three to five days.

To investigate an alternative method for improving the strength of interior column-slab joints, specimen B-3 was provided with a high-strength concrete core. During casting of the slab, a 75 by 75 mm core inside the column reinforcing cage was blocked out. This core region was filled with high-strength concrete while casting the upper column stub. The advantage of this construction scheme is that it avoids using two different grades of concrete while casting the slab.

The column and slab concrete was batched in the lab using local aggregates and type 10 cement. The coarse aggregate had a maximum size of 14 mm. Silica fume and superplasticizer were used in the high-strength column concrete. All reinforcement had a nominal yield strength of 400 MPa.

A sketch of the setup for testing column-slab joints with loaded slabs is shown in Fig. 6. The slab loads were applied with four geometrically similar center-hole jacks connected to a common manifold and controlled with a single hand pump. The main column load was applied using a universal testing machine with a nominal capacity of 6,500 kN.

Instrumentation and Control

All data were recorded electronically. The main column load was applied under stroke control using a built-in ramp function. The column load was measured with a differential pressure-type load cell in the universal test machine. Slab loads were controlled manually and measured by means of individual load cells placed in series with each jack.

Column strains were measured above, below, and through the thickness of the slab. In addition, electrical resistance strain gauges were mounted on the slab and column reinforcement. Figure 5 shows the layout of strain gauges on the slab rein-

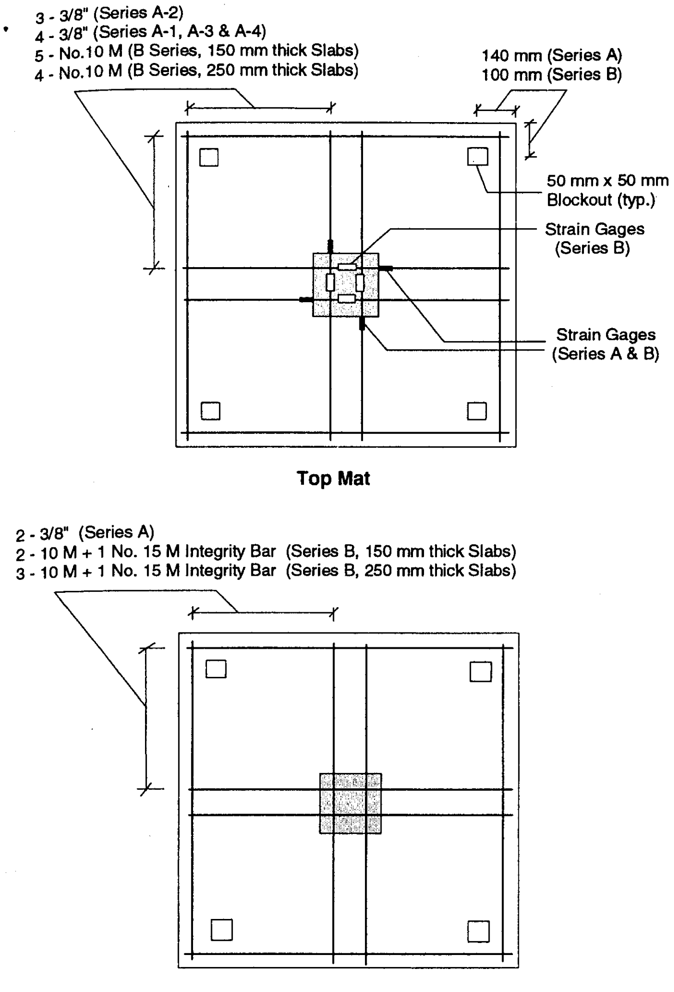

FIG. 5. Slab Reinforcement and Strain Gauge Layouts

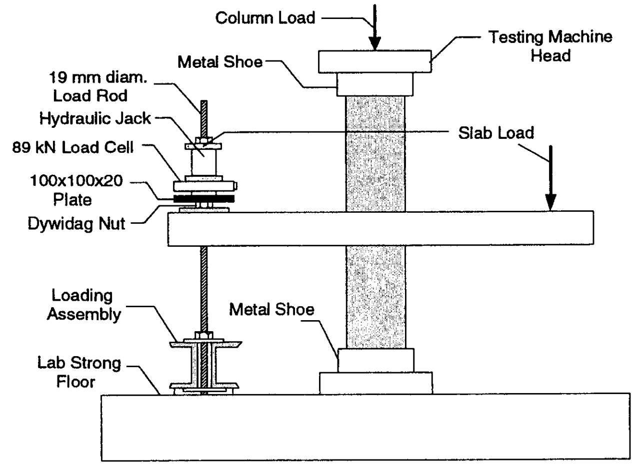

FIG. 6. Test Setup

forcement. For each specimen of series A, four strain gauges were mounted on the top mat reinforcing bars at the column face. The output of these gauges was used to determine the appropriate slab load for each specimen. Each specimen in series B had a total of 16 electrical resistance strain gauges: four on the slab top steel at the column face, as in series A, four on the slab top steel on the centerline of the specimen, and eight on the column steel.

Testing Procedure

All specimens were initially loaded with 200 to 400 kN to seat the specimen and to ensure that all gauges were functioning. At this point, the full slab load, if any, was applied to the slab. This slab load was held constant while the column load was increased to failure.

In series A, the target slab load was determined by gradually increasing the load until the average output of the four strain gauges on the slab reinforcement at the column face matched the target value. The selected target values of strain were 0, 1,000$\mu\varepsilon$, and 2,000$\mu\varepsilon$. The total slab load was recorded and maintained for the remainder of the test. For typical column supported slabs, a strain of 1,000$\mu\varepsilon$ is consistent with dead load only. A strain of 2,000$\mu\varepsilon$ is consistent with full service live and dead load.

In series B, the target value for slab load was based on an analysis at average service load conditions. After applying the initial seating load on the column, the slab was loaded to its predetermined target value. In most cases, the average slab strain at this predetermined level of load was about 1,500$\mu\varepsilon$.

In this investigation, the applied slab loads are all consistent with service levels of load. In a column-supported flat slab or plate, strain in the slab flexural reinforcement at the face of the column is very high. One would expect a strain of about 1,000$\mu\varepsilon$ under dead load alone. A strain of 2,000$\mu\varepsilon$ is consistent with full service live and dead load on the slab.

In all cases, the loading regime simulated the combination of an extreme event on the column with some level of service load on the slab. There is scope for additional experimental work simulating an extreme loading event on the slab with average service load on the column.

TEST RESULTS

Test results for all specimens are reported in Table 3. The term P_{test} corresponds to the maximum compressive load applied on the column. The term ε_{init} refers to the initial strain in the slab top reinforcement measured at the column face. The term P_{slab} corresponds to the total slab load maintained throughout the tests. This value is equal to the sum of the four point loads applied on each corner of the slab segments. The effective compressive strength values, f'_{ce}, were calculated according to (2) taking α_1 equal to 0.85.

BEHAVIOR OF TEST SPECIMENS

The interior column-slab joints with unloaded slabs behaved like the specimens tested by Bianchini et al. (1960) and Gamble and Klinar (1991). Fig. 7 illustrates a typical crack pattern of an interior joint without slab load. Cracking in the slab was first observed when the applied column stress exceeded the cylinder strength of the joint concrete. At this level, the column longitudinal bars yielded in the joint region. As the test progressed, cracks radiated from the column toward the slab edges. Then, cracks formed at the middle edges of the slab and progressed toward the column. All these cracks were through the full slab thickness.

The column stubs remained uncracked nearly until ultimate load. At this point, splitting cracks penetrated either the upper or lower column stubs. Whether the cracks penetrated the upper or lower column stub depended upon the degree of restraint offered locally by the slab reinforcement. Most slabs had more top steel than bottom steel, and in these cases, the cracking penetrated the lower column stub. The greater stiffness of the top mat caused the slabs of these specimens to curl upwards slightly. Gamble and Klinar also reported this effect.

The cracking behavior of the specimens with slab loads was markedly different. A typical crack pattern for a slab-loaded specimen is shown in Fig. 8. When the slab was loaded, flexural cracks formed on the top surface directly above the reinforcing bars and extended from the column to the slab edges. Column reinforcement in the joint yielded when the applied

TABLE 3. Test Results

Series (1)	Specimen (2)	h/c (3)	P_{test} (kN) (4)	P_{slab} (kN)^a (5)	f'_{ce} (MPa)^b (6)	ε_{init} ($\mu\varepsilon$)^c (7)	f'_{cc}/f'_{cs} (8)	f'_{ce}/f'_{cs} (9)
A	A1-A	0.5	3,914	0	100.31	0	2.63	2.51
A	A1-B	0.5	3,678	48	93.08	1,000	2.63	2.33
A	A1-C	0.5	3,498	94	87.56	2,000	2.63	2.19
A	A2-A	0.5	3,820	0	97.43	0	2.43	2.12
A	A2-B	0.5	3,807	33.2	97.03	1,000	2.43	2.11
A	A2-C	0.5	3,591	86	90.41	2,000	2.43	1.97
A	A3-A	0.75	3,437	0	85.69	0	3.56	3.43
A	A3-B	0.75	3,174	100	77.63	1,000	3.56	3.11
A	A3-C^d	0.75	2,275	157.2	50.09	2,000	3.56	2.00
A	A4-A	0.75	3,272	0	80.64	0	4.61	3.51
A	A4-B	0.75	2,927	93.2	70.07	1,000	4.61	3.05
A	A4-C	0.75	2,376	135.2	53.19	2,000	4.61	2.31
B	B-1	1.0	4,072	173.2	71.54	750	2.48	1.70
B	B-2	0.6	5,359	130	96.08	1,600	2.48	2.29
B	B-3	1.0	5,078	173.2	90.72	600	2.57	2.06
B	B-4	0.6	6,298	0	113.99	0	2.57	2.59
B	B-5	1.0	2,703	173.2	45.44	1,500	6.33	3.03
B	B-6	0.6	3,720	130	64.83	2,000	6.33	4.32
B	B-7^e	0.7	2,758	173.2	47.45	1,200	6.32	2.50
B	B-8^e	1.17	4,032	130	72.25	1,800	6.32	3.80

[a]Reported slab load values correspond to the sum of the four point loads applied on the slab.
[b]Values calculated based on Eq. (2).
[c]Average strain in top slab reinforcement at column fact right after the slab load was applied.
[d]Specimen exhibited premature anchorage failure in the slab.
[e]The h/c ratio for these two specimens was calculated based on the shorter column dimension.

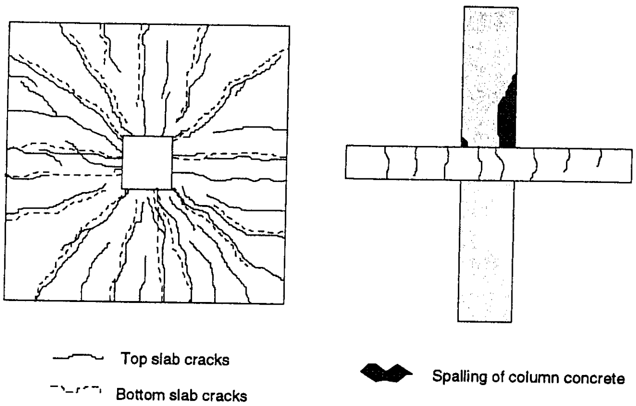

FIG. 7. Cracking Pattern: Specimen B-4 (Unloaded Slab)

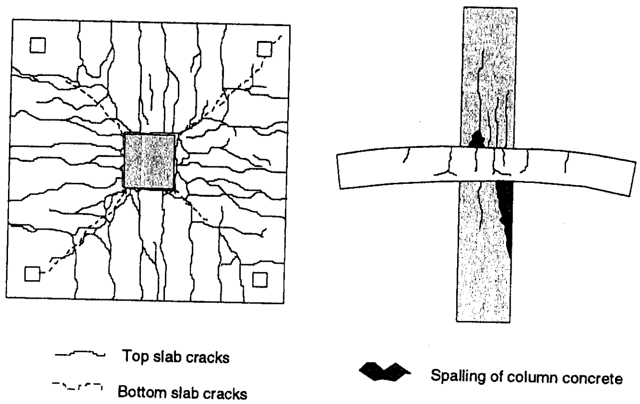

FIG. 8. Cracking Pattern: Specimen B-2 (Loaded Slab)

stress reached the cylinder strength of the joint concrete. At this point and for the remainder of the test, it was necessary to frequently adjust the jacks loading the slab to maintain constant load. Failure to do so resulted not only in a decrease in the level of slab load but also in an increase in the applied column load. A reduction in slab load improved the confinement of the column-slab joint, thereby increasing both the strength and stiffness of the joint.

After yielding of the slab reinforcement, cracks formed at the face of the top column stub. As the test progressed, these cracks opened, suggesting that the slab concrete provided little or no restraint to the upper portion of the joint. Ultimately, splitting cracks extended mainly into the top column stub since much more restraint was provided to the lower half of the joint by the flexural compression block of the slab.

The nature of the failure depended upon whether it occurred inside or outside of the joint. In cases where failure was controlled by crushing within the joint, there was considerable softening behavior. In a few cases, however, the strength of the joint approached that of the high-strength column. Failure of these specimens was explosive.

JOINT STRESS-STRAIN BEHAVIOR

Fig. 9 shows the longitudinal stress-strain behavior of a typical column-slab joint with a loaded slab, specimen B-6. The plotted stress values correspond to the average applied concrete compressive stress, calculated as

$$f_c = \frac{P_{col} - f_s A_{st}}{(A_g - A_{st})}, \; f_s \le f_y \tag{6}$$

For comparison, stress-strain curves obtained from cylinder tests of the slab and column concrete are given. Note that, by definition, the peak value of stress in the joint concrete is 85% of f'_{ce}.

At levels of stress below the uniaxial compression strength of the concrete, the stress-strain behavior of the joint concrete is reasonably close to that obtained from a cylinder test. There is a marked change in the slope of the stress-strain curve at a stress corresponding to the unconfined compression strength of the joint concrete. Comparing the behavior of the joint with that of the corresponding cylinder test clearly shows the effect of the confinement from the surrounding slab. The ultimate stress and strain of the joint are greatly increased over those obtained from the cylinder. Outside of the joint, the stress-strain behavior of the column concrete remained elastic and

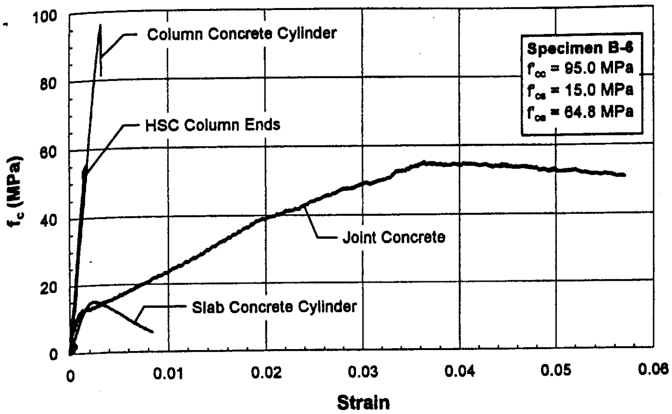

FIG. 9. Stress-Strain Behavior (Specimen B-6)

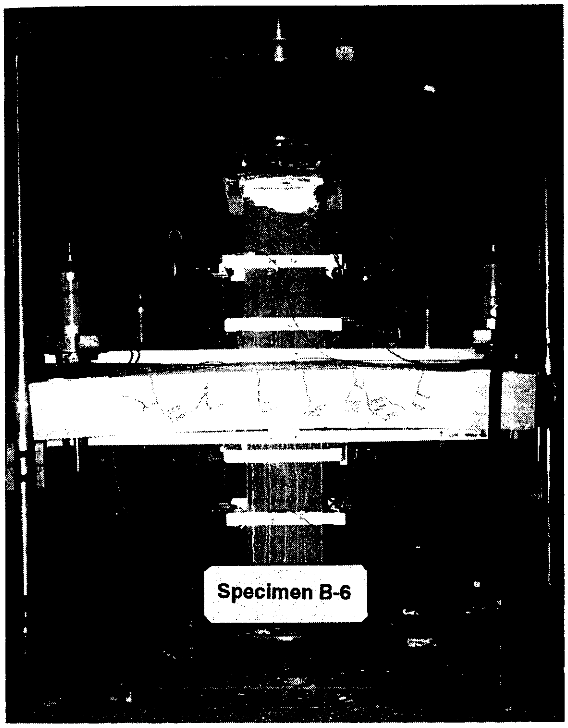

FIG. 10. Test of Specimen B-6 (Loaded Slab)

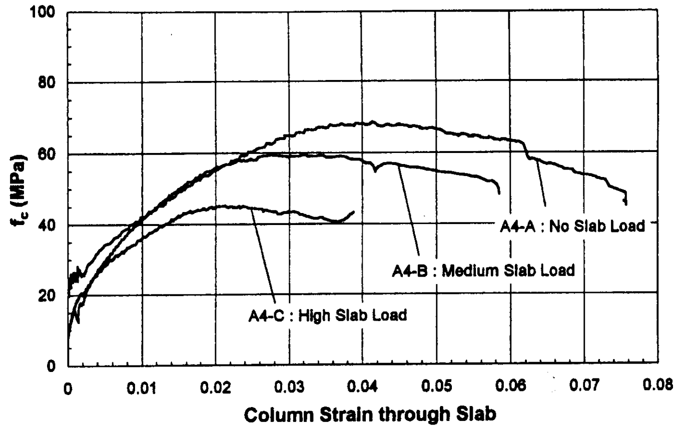

FIG. 11. Effect of Slab Load on Interior Joint Strength

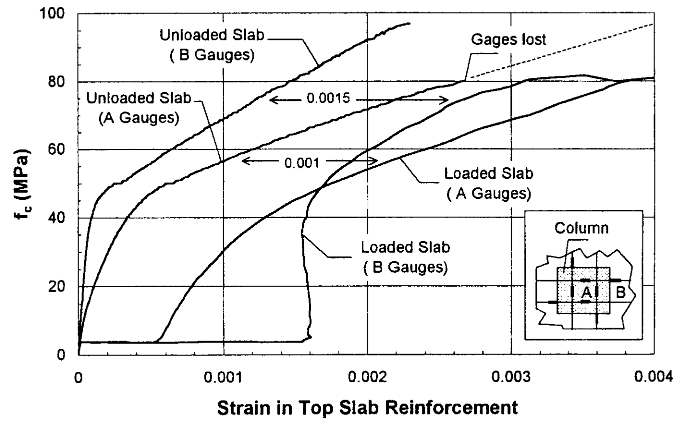

FIG. 12. Effect of Slab Load on Joint Transverse Strain

matched that obtained from a cylinder test. Fig. 10 shows a photograph of specimen B-6 during testing.

Effect of Slab Load

The joint stress-strain behavior confirms that specimens with loaded slabs behave differently than those without slab loads. Fig. 11 compares the stress-strain curves of specimens A4-A, A4-B, and A4-C.

The effect of the slab loads is to reduce both the maximum compressive stress and the strain at peak stress. For these specimens the strain at peak stress ranged from 2% to 4%. These values are 10 to 20 times greater than those associated with unconfined compression, typically equal to 0.2%. This shows that even when high slab load intensities are applied, the joint benefits from some confinement.

Fig. 12 compares the joint transverse strains at the column face and at the column centerline of two interior column-slab joints with and without slab loads. Transverse strains were obtained from gauges placed on the top slab reinforcement and are plotted with tension positive. For the specimen without slab load (B-4), the strain at the face of the joint is always less than that at the center. For the slab-loaded specimen (B-2), the strain at the face of the joint is higher than at the joint center right after the slab loads have been applied. Over the course of the test, however, the strain at the centerline increases faster than it does at the column face. The former overtakes the latter when the applied stress exceeds the cylinder strength of the slab concrete and the column longitudinal reinforcement yields within the joint. Beyond this level, both strain readings increase in tandem.

One striking observation from Fig. 12 is that strains of the specimen with the loaded slab virtually parallel those of the specimen with the unloaded slab. The effect of slab loading was to increment the transverse tensile strain by about 1,000$\mu\varepsilon$ at the column centerline, and by about 1,500$\mu\varepsilon$ at the column face. This suggests that the upper half of an interior column-slab joint is pulled apart by the bending action of the slab.

The tests reported here model service load on the slab combined with an extreme load event on the column. Because the tests do not allow for moment redistribution within the slab, they may exaggerate the effect of slab load. In a continuous slab, negative bending moment at the columns can redistribute to positive moment, thereby relieving the top mat slab reinforcement in the vicinity of the column. However, if one considers instead average service load on the column combined with an extreme load event on the slab, there is little benefit from redistribution.

Effect of Slab and Column Dimensions

The gross geometry of a joint is described by its aspect ratio, h/c, where h is the slab thickness and c is the column dimension. Fig. 13 illustrates the effect of varying the aspect ratio with data from four test specimens with two different ratios of column to slab concrete strength. The strength of the column decreases as h/c increases. The reduction is higher for the specimens with larger ratio of column to slab concrete strength.

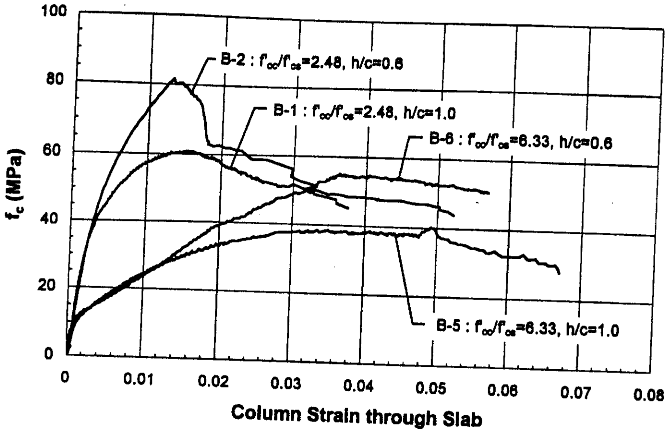

FIG. 13. Effect of *h/c* on Interior Joint Strength

In many cases, the joint aspect ratio will be less than 1/2 and often less than 1/3. However, joint aspect ratios of the order of unity or more are not unreasonable for slabs with drop panels or for joints with rectangular columns. In the case of rectangular columns, it will be shown that the smaller column dimension governs the aspect ratio of the joint.

Effect of HSC Core in Joint Region

Fig. 14 compares the stress-strain curves of two specimens, B-1 and B-3. These specimens had the same dimensions and were built using similar slab and column concrete. Both were tested with loaded slabs. Specimen B-3 had a core of high-strength column concrete in the joint region, while B-1 had slab concrete throughout the joint region. Although the area of the high-strength core accounted for 9% of the cross-sectional area of the column, specimen B-3 reached an ultimate average stress that was 21.1% higher than B-1. This suggests that the longitudinal stress distribution in the joint is nonuniform, with the high-strength core carrying a disproportionate fraction of the total applied load. The high-strength core in specimen B-3 extended the full thickness of the slab. However, because the flexural compression block confines the lower part of the joint, it may be sufficient to place a high-strength core only in the top portion of the joint.

EFFECTIVE STRENGTH OF COLUMN-SLAB JOINTS

Fig. 15 shows the relationship between the effective strength ratio, f'_{ce}/f'_{cs}, and the joint strength ratio, f'_{cc}/f'_{cs}, for specimens with unloaded slabs. For comparison, the design equations of the ACI (1995) and Canadian (1994) standards and Gamble and Klinar (1991) are given.

Fig. 15 shows that test results on interior joint specimens without slab loads reported in this study are consistent with those available in the literature. It also shows that the design equation for f'_{ce} given in the ACI code may overestimate the effective strength of joints with high aspect ratios. On the other hand, the design equation in the Canadian standard appears to be conservative for all results shown. The design limit proposed by Gamble and Klinar appears to be a reasonable lower bound for the results.

The measured effective strengths obtained from the specimens of series A are shown in Fig. 16. In all cases, specimens with load applied to the slabs failed at lower effective strengths than did their companion specimens with no slab load. As would be expected, specimens with the highest slab loads (2,000$\mu\varepsilon$) had the greatest reduction in effective strength.

Fig. 16 shows that, for column-slab joints with loaded slabs, the ACI code equation is not conservative, particularly for high f'_{cc}/f'_{cs} ratios. This is highlighted by the performance of specimen A-4C, an interior plate with heavy slab loads. For this specimen the effective strength predicted by the 1995 ACI code is 65% higher than the measured effective strength. The design equation for interior columns given in CSA A23.3-94 appears to be conservative for all results shown.

Fig. 17 shows the effects of joint aspect ratio, *h/c*, and column rectangularity on the compressive strength of interior columns. As would be expected, the effective compressive strength of an interior column decreases as *h/c* increases. The expression for effective strength given by CSA A23.3-94 is a good predictor of the results for the two square specimens with an aspect ratio of unity, B-1 and B-5. The results for specimens B-2 and B-6, each with an aspect ratio of 0.6, approach the effective strengths predicted by the ACI code.

The joint aspect ratio for a specimen with a rectangular column lies between two limiting values, one defined by the smaller column dimension and the other defined by the larger

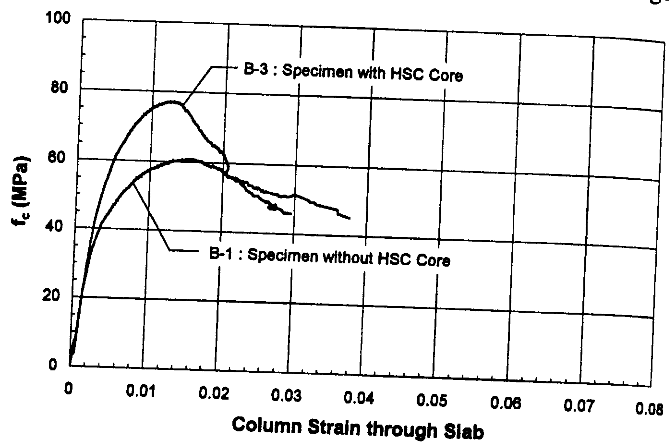

FIG. 14. Effect of High-Strength Core on Joint Strength

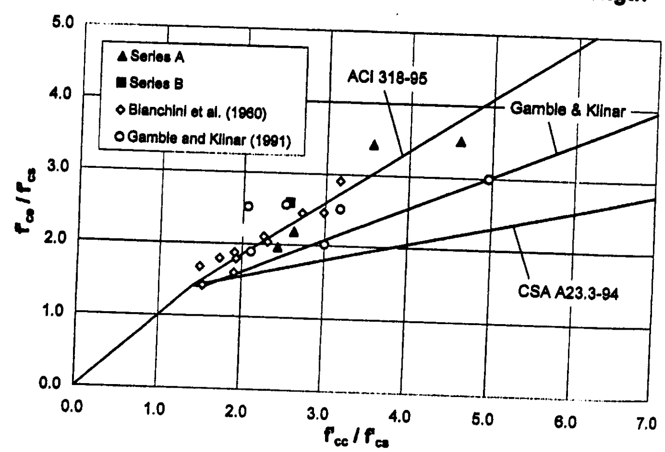

FIG. 15. Results of Tests with Unloaded Slabs

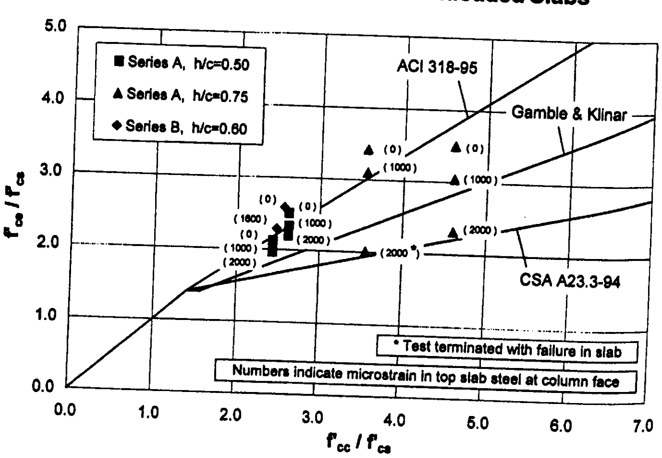

FIG. 16. Effect of Slab Load on Interior Joint Strength

column dimension. As shown in Fig. 17, both specimens with rectangular columns, B-7 and B-8, had effective stress ratios about 15% lower than did the corresponding test specimens with square columns, B-5 and B-6. This reduction in effective stress ratio is consistent with an increase in the joint aspect ratio. This implies that the shorter column dimension should be used in calculating h/c for a rectangular column.

RECOMMENDED DESIGN PROVISIONS FOR INTERIOR COLUMNS

In all available tests, the addition of slab load reduces the effective strength of interior column-slab joints. This implies that, had any realistic amount of slab load been applied to the specimens tested by Bianchini et al. and Gamble and Klinar, the measured effective compressive strengths would have been smaller than those reported. Consequently, design provisions for interior columns must be based on experimental results of joint specimens with loaded slabs.

There appears to be no reason to abandon the basic format of either the ACI or CSA provisions. Both codes define a bilinear relationship between the effective strength ratio, f'_{ce}/f'_{cs}, and the joint concrete strength ratio, f'_{cc}/f'_{cs}. It is essential, however, that the design equation for estimating the effective strength of the joint concrete account for the aspect ratio of the joint, h/c. The following design equation is proposed for column-slab joints:

$$\frac{f'_{cc}}{f'_{cs}} \leq 1.4; \quad f'_{ce} = f'_{cc} \tag{7a}$$

$$\frac{f'_{cc}}{f'_{cs}} > 1.4; \quad f'_{ce} = \left(\frac{0.25}{h/c}\right) f'_{cc} + \left(1.4 - \frac{0.35}{h/c}\right) f'_{cs} \tag{7b}$$

with h/c not to be taken less than 1/3. For a joint with a rectangular column, c is taken as the smaller column dimension.

For any given aspect ratio, (7) produces a bilinear relationship between the effective and the joint concrete strength ratios, as shown in Fig. 18. Because existing design provisions appear to be adequate for lower values of joint concrete strength ratios, the first segment of the bilinear relationship follows the provisions in both the ACI and CSA codes. If the joint concrete stress ratio is less than 1.4, the effective strength of the joint is set equal to the strength of the column concrete. The slope of the second segment depends on the joint aspect ratio; the slope increases as the aspect ratio decreases. This means that as the slab becomes thin relative to the column dimension, slab loading has less of an effect on the effective strength of the column-slab joint. When the joint aspect ratio

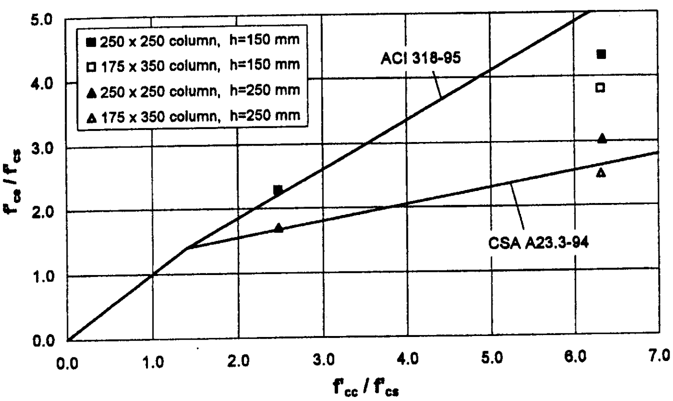

FIG. 17. Effect of h/c and Column Rectangularity on Interior Joint Strength

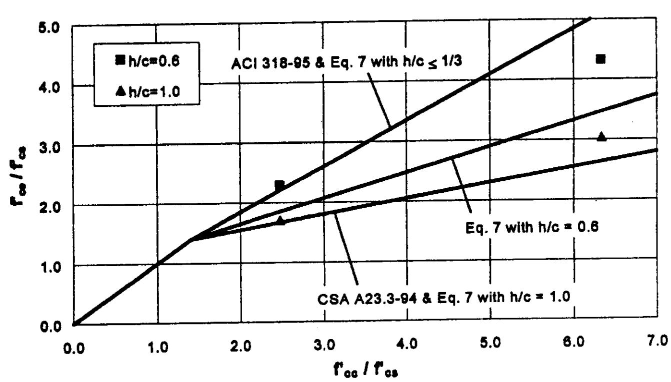

FIG. 18. Comparison of Test Results with Proposed Design Provisions

TABLE 4. Ratios of Test-to-Predicted Column Effective Strength, f'_{ce}

Specimen		ACI 318-95		CSA A23.3-94		Authors	
Mark (1)	$f_{ce,test}$ (2)	$f'_{ce,calc}$ (3)	$f'_{ce,test}/f'_{ce,calc}$ (4)	$f'_{ce,calc}$ (5)	$f'_{ce,test}/f'_{ce,calc}$ (6)	$f'_{ce,calc}$ (7)	$f'_{ce,test}/f'_{ce,calc}$ (8)
A1-B	93.08	92.75	1.00	68.25	1.36	80.50	1.16
A1-C	87.56	92.75	0.94	68.25	1.28	80.50	1.09
A2-B	97.03	100.1	0.97	76.3	1.27	88.20	1.10
A2-C	90.41	100.1	0.90	76.3	1.18	88.20	1.03
A3-B	77.63	75.5	1.03	48.5	1.60	53.00	1.46
A3-C[a]	50.09	75.5	0.66	48.5	1.03	53.00	0.95
A4-B	70.07	87.55	0.80	50.65	1.38	56.80	1.23
A4-C	53.19	87.55	0.61	50.65	1.05	56.80	0.94
B-1	71.54	92.70	0.77	70.10	1.02	70.10	1.02
B-2	96.08	92.70	1.04	70.10	1.37	77.63	1.24
B-3	90.72	100.15	0.91	74.45	1.22	74.45	1.22
B-5	45.44	76.50	0.59	39.50	1.15	39.50	1.15
B-6	64.83	76.50	0.85	39.50	1.64	51.83	1.25
B-7	47.45	96.65	0.49	49.95	0.95	42.93	1.11
B-8	72.25	96.65	0.75	49.95	1.45	53.75	1.34
Mean			0.82		1.26		1.15
Standard deviation			0.172		0.208		0.145
C.O.V.			20.9%		16.4%		12.6%

Note: Results for A1-A, A2-A, A3-A, A4-A, and B-4 are not reported since no slab load was applied on these specimens. Light slab loads were applied on A1-B, A2-B, A3-B, and A4-B. Heavy slab loads were applied on A1-C, A2-C, A3-C, and A4-C. Slab loads applied on B-1 to B-8 (excluding B-4) simulated service load conditions.

[a]Specimen exhibited premature anchorage failure in slab.

is less than or equal to 1/3, the design curve is the same as that given in the 1995 ACI code. For a joint aspect ratio of 1.0, the expression matches that given in the 1994 Canadian standard.

Table 4 compares the proposed design equation with the provisions in the ACI and Canadian standards using the results from tests with loaded slabs. With an average test to predicted ratio of 0.82, the ACI procedure consistently errs on the unsafe side, overestimating the effective strength of slab-column joints. In some cases, the error is substantial. Specimen B-7 failed at just less than half the load that one would predict using the ACI code. In contrast, the procedure in the Canadian standard is excessively conservative, particularly for joints with relatively thin slabs, such as B-6. The proposed design equation is more reliable and accurate than either the ACI or CSA design equations. With an average test to predicted ratio of 1.15 and a coefficient of variation of 12.6%, the proposed equation yields consistently safe results without being excessively conservative.

SUMMARY AND CONCLUSIONS

Twenty reinforced concrete interior column-slab connection specimens were tested to study the transmission of column loads through floors built with weaker concrete.

1. Test results show that slab loading reduces the effective strength of a column-slab joint. Since some level of slab load is inevitable in any practical structure, it is imperative that the design of column-slab joints be based on experimental results in which slabs are loaded.
2. The effective strength of a column-slab joint is influenced by its aspect ratio, *h/c*. As the aspect ratio increases (i.e., the slab becomes thicker relative to the column dimension), the effective strength of the joint decreases.
3. The controlling aspect ratio of a joint between a slab and a rectangular column is based on the minimum column dimension.
4. The expression for the effective concrete strength of an interior column-slab joint given in the 1995 ACI code is unsafe for joints with high aspect ratio.
5. The expression for the effective concrete strength of an interior column-slab joint given in the 1994 Canadian standard is excessively conservative for joints with low aspect ratios.
6. A new expression for predicting the effective strength of column-slab joints is proposed. The expression is shown to be more reliable and accurate than existing design equations.
7. Placing a high-strength concrete core in the joint region enhances the compressive strength of the connection. This procedure, or some variation, may provide a practical solution that maintains the strength of the column-slab joint while avoiding the construction problems associated with "pudding." More experimental research is needed to evaluate this procedure.
8. Tests in the present investigation simulated an extreme loading event on the column with service load on the slab. This load combination is more consistent with existing tests of specimens with unloaded slabs. However, there may be a greater structural risk associated with an extreme loading event on the slab combined with service load on the column. Future work should examine column-slab joint behavior under such load combinations.

ACKNOWLEDGMENTS

Funding for this research was provided by the Minister of State, Science and Technology through Concrete Canada, part of the Networks of Centres of Excellence Program. Cement was donated by Inland Cement and by LaFarge. Chemical and mineral admixtures were donated by Master Builders Technologies and by W. R. Grace and Company. The writers gratefully acknowledge this support.

APPENDIX I. REFERENCES

Bianchini, A. C., Woods, R. E., and Kesler, C. E. (1960). "Effect of floor concrete strength on column strength." *ACI J.*, 31(11), 1149–1169.

"Building code requirements for structural concrete and commentary." (1995). *ACI 318-95*, American Concrete Institute (ACI), Detroit, Mich., 369 pp.

"Design of concrete structures." (1994). *CSA A23.3-94*, Canadian Standards Association, Rexdale, Ont., Canada.

Gamble, W. L., and Klinar, J. D. (1991). "Tests of high-strength concrete columns with intervening floor slabs." *J. Struct. Engrg.*, ASCE, 117(5), 1462–1476.

Ospina, C. E., and Alexander, S. D. B. (1997). "Transmission of high-strength concrete column loads through concrete floors." *Struct. Engrg. Rep. No. 214*, Dept. of Civ. Engrg., Univ. of Alberta, Edmonton, Canada.

APPENDIX II. NOTATION

The following symbols are used in this paper:

A_g = column gross section, mm^2;
A_{st} = area of column longitudinal reinforcement, mm^2;
c = column dimension, mm;
f_c = average column compressive stress, MPa;
f'_c = specified cylinder compressive strength of concrete, MPa;
f'_{cs} = cylinder compressive strength of slab concrete, MPa;
f'_{cc} = cylinder compressive strength of column concrete, MPa;
f'_{ce} = column effective compressive strength, MPa;
f_s = stress in column longitudinal reinforcement, MPa;
f_y = yield strength of column longitudinal reinforcement, MPa;
h = slab thickness, mm;
P_{slab} = total vertical slab load maintained through the test, kN;
P_{test} = maximum compressive column load applied in the test, kN;
α_1 = ratio of stress in rectangular stress block to cylinder strength; and
ε_{init} = longitudinal strain in slab top reinforcement at column face.